False Alarm Analysis of the CATM-CFAR in Presence of Clutter Edge

Dejan IVKOVIĆ [1], *Milenko ANDRIĆ* [2], *Bojan ZRNIĆ* [3]

[1] Military Technical Institute, Ratka Resanovića 1, 11030 Belgrade, Serbia
[2] University of Defense, Generala Pavla Jurišića Šturma 33, 11000 Belgrade, Serbia
[3] Defense Technologies Department, Nemanjina 15, 11000 Belgrade, Serbia

divkovic555@gmail.com, asmilenko@beotel.net, bojan.zrnic@vs.rs

Abstract. *This paper presents a false alarm analysis of the cell-averaging-trimmed-mean constant false alarm rate (CATM-CFAR) detector in the presence of clutter edge. Structure of the CATM-CFAR detector is described briefly. Detection curves for optimal, CATM, cell-averaging (CA), trimmed-mean (TM) and ordered-statistic (OS) CFAR detectors has been analyzed and compared for desired probability of false alarm and determined size of the reference window. False alarm analysis of the CATM-CFAR in case of clutter with constant clutter-to-noise ratio has been conducted. Also, comparative false alarm analysis of CATM and some of well known CFAR detectors is carried out and results are presented.*

Keywords

CFAR detection, false alarm rate, clutter edge.

1. Introduction

Radar works always in an environment with different sources of noise. It seeks for use of the adaptive threshold detector, which has a feature that adjusts automatically its level according to variety of the interference power in order to maintain a constant false alarm rate. Detector in radar receivers with this feature is known as the constant false alarm rate (CFAR) processor.

In a general CFAR processor, the square-law detected signal is sampled in range for every range bin. The range samples are sent serially into a shift register of length $N + 1 = 2n + 1$ as shown in Fig. 1. The leading n samples and the lagging n samples constitute the reference window. The data available in the reference window are processed to obtain the statistic Z that is the estimate of the total noise power. To maintain the probability of false alarm (P_{fa}) at a desired constant value when the total background noise is homogeneous, the detection threshold is obtained by scaling the statistic Z with a scale factor T.

The three most important parameters of any type of CFAR detectors are:

- probability of detection P_d for a given value of signal-to-noise ratio *SNR*,
- average decision threshold *ADT* [1] and
- clutter edge properties.

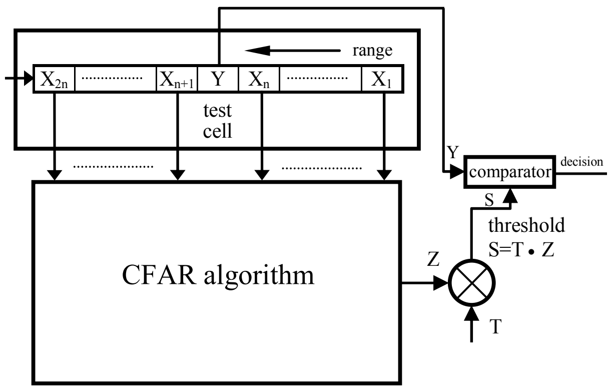

Fig. 1. Typical CFAR detector.

Some CFAR algorithm is better than others if it provides a greater probability of detection for a given value of signal-to-noise ratio, lower average decision threshold and as low as possible probability of false alarm deviations from the desired values.

In much practical application, the clutter returns may not be uniformly distributed. In the presence of clutter edge the cell-averaging (CA-CFAR) detector performance can degrade significantly. To alleviate this problem the greatest-of CFAR (GO-CFAR) detector was proposed [2, 3]. In the GO-CFAR detector the leading and lagging reference samples are separately summed and the larger of the two is used to set a threshold. GO-CFAR and ordered-statistic CFAR (OS-CFAR) behaviors in the presence of clutter edge are analyzed in [1]. With respect to clutter, two signal situations were discussed: clutter amplitudes are statistically independent and Rayleigh distributed; clutter is represented by a constant amplitude response. Features of trimmed mean CFAR (TM-CFAR) detector [4] in regions of clutter transitions are presented in [5]. By judiciously trimming the ordered samples, the TM-CFAR detector may actually perform to some extent better than the OS-CFAR detector in presence of clutter edge. The weighted order statistic and fuzzy rules CFAR (WOSF-CFAR) [6] detector uses some soft rules based on fuzzy logic to cure the mentioned clutter edge problems. A method for automatic clutter edge localization is proposed in [7], achieving elimination of the misleading data and improving of the CFAR detection performances.

In this paper, the emphasis is on the false alarm analysis in presence of clutter edge of cell-averaging-trimmed-mean constant false alarm rate (CATM-CFAR) detector, which is proposed in [8]. The paper is organized as follows. In Section 2, a short description of CATM-CFAR is given, and exact expressions for parameters of this CFAR model are presented. Results of false alarm analysis for CATM-CFAR are showed in Section 3. In Section 4, a comparison CATM-CFAR with two other models of CFAR detector in presence of clutter edge is done. Finally, in Section 5, we gave some conclusions.

2. CATM-CFAR Detector

The cell-averaging-trimmed-mean CFAR (CATM-CFAR) detector [8] optimizes good features of two CFAR detectors depending on the characteristics of clutter and present targets with the goal of increasing the probability of detection under constant probability of false alarm rate. It is realized by parallel operation of two types of CFAR detector: cell-averaging CFAR (CA-CFAR) [3] and TM-CFAR. Its structure is shown in Fig. 2.

CA-CFAR detector and TM-CFAR detector work simultaneously and independently but with the same scaling factor of the detection threshold T. They produce own mean clutter power level Z using the appropriate CFAR algorithm. Next, they calculate own detection thresholds S_{CA} and S_{TM}. After comparison with the content in cell under test Y, they decide about target presence independently. The finite decision about target presence is made in fusion center which is composed of one "and" logic circuit. If the both input single decision in the fusion center are positive, the finite decision of the fusion center is presence of the target in cell under test. In each other cases finite decision is negative and target is not declared at the location which corresponds with cell under test.

Expressions for probability of false alarm P_{fa}, probability of detection P_d and average decision threshold ADT for CATM-CFAR are derived in [8] in detail. Because of that, we give only final expressions here:

$$P_{fa} = (1+T)^{-N} \prod_{i=1}^{N-T_1-T_2} M_{V_i}(T), \tag{1}$$

$$P_d = \left(1+\frac{T}{1+SNR}\right)^{-N} \prod_{i=1}^{N-T_1-T_2} M_{V_i}\left(\frac{T}{1+SNR}\right), \tag{2}$$

$$ADT = TN + \frac{TN!}{(N-T_1-1)!} \sum_{j=0}^{T_1} \frac{(-1)^{T_1-j}}{(N-j)\,j!\,(T_1-j)!} \cdot \left[\frac{N-T_1-T_2}{N-j} + \sum_{i=2}^{N-T_1-T_2} \frac{1}{a_i}\right] \tag{3}$$

where T_1 is the number of discarded smallest ranked cells, T_2 is the number of discarded greatest ranked cells in the reference window. Auxiliary variables M_V and a are determined as follow:

$$M_{V_1}(T) = \frac{N!}{T_1!(N-T_1-1)!(N-T_1-T_2)} \cdot \sum_{j=0}^{T_1} \frac{\binom{T_1}{j}(-1)^{T_1-j}}{\frac{N-j}{N-T_1-T_2}+T}, \tag{4}$$

$$M_{V_i}(T) = \frac{a_i}{a_i+T}, \quad i = 2,3,\ldots,N-T_1-T_2\,, \tag{5}$$

$$a_i = \frac{N-T_1-i+1}{N-T_1-T_2-i+1}. \tag{6}$$

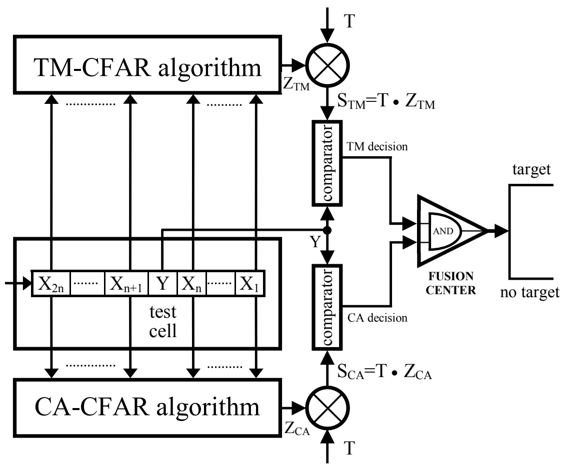

Fig. 2. Block diagram of CATM-CFAR detector.

In Tab. 1 the scaling factor of the detection threshold T and average decision threshold ADT of the CATM-CFAR detector for symmetric and asymmetric trimming for P_{fa}= 10^{-6} and N = 24 are listed. Values of T are calculated iteratively from (1) for given values of T_1 and T_2. Values of ADT are computed from (3).

Symmetric trimming				Asymmetric trimming			
T_1	T_2	T	ADT	T_1	T_2	T	ADT
0	0	0.333	16.0090	2	4	0.441	16.3708
1	1	0.364	16.0833	2	7	0.513	16.7155
2	2	0.391	16.1727	2	10	0.582	17.1159
3	3	0.418	16.2702	2	15	0.687	17.8563
4	4	0.445	16.3770	2	17	0.721	18.1440
5	5	0.473	16.4956	2	20	0.761	18.5099
6	6	0.502	16.6312	4	2	0.394	16.1757
7	7	0.534	16.7900	7	2	0.403	16.1890
8	8	0.569	16.9822	10	2	0.418	16.2241
9	9	0.608	17.2246	15	2	0.469	16.4007
10	10	0.653	17.5453	17	2	0.506	16.5728
11	11	0.708	17.9952	20	2	0.609	17.2001

Tab. 1. Scaling factor T and average decision threshold ADT of CATM-CFAR detector (P_{fa}=10^{-6}, N=24).

Probability of detection of optimal detector and some CATM-CFAR detector as a function of the signal-to-noise ratio for parameter values from Tab. 1 are shown in Fig. 3 and Fig. 4. The notation CATM(T_1,T_2) stands for CATM-CFAR with lower trimming T_1 and upper trimming T_2.

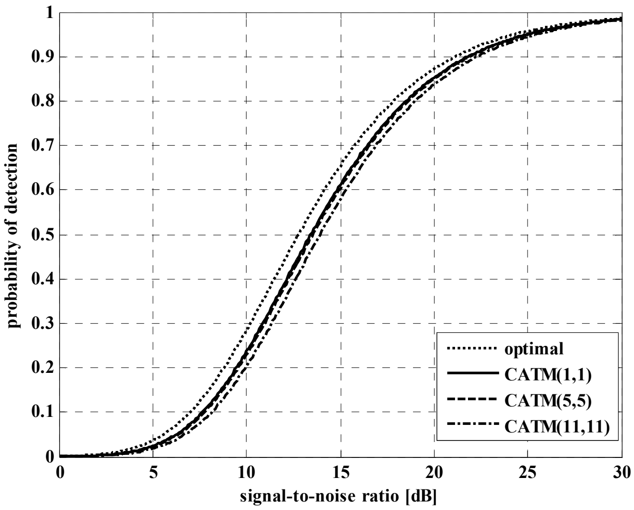

Fig. 3. Detection curves for optimal and symmetric trimming CATM-CFAR detectors (P_{fa} = 10^{-6}, N = 24).

Probability of detection of theoretically optimal detector P_{dO} is calculated according to expression [8]:

$$P_{dO} = P_{fa}^{(1+SNR)^{-1}}. \tag{7}$$

In Fig. 3 it can be seen that with the increase of number of discarded cells for symmetric trimming CATM-CFAR there is a decrease of probability of detection. This phenomenon is evident in case of the asymmetric trimming CATM-CFAR also, and Fig. 4 shows this. By selecting the area for the probability of detection around the value of 0.5 (Fig. 5), it can be concluded that the loss in the asymmetric trimming CATM-CFAR is smaller when T_1 is less than T_2. Approximate signal-to-noise ratio losses Δ_O for mentioned asymmetric trimming CATM-CFAR in relation to optimal detector are listed in Tab. 2. Values for Δ_O were calculated for P_d = 0.5 and P_{fa} = 10^{-6}, according to the following expression [8]:

$$\Delta_O = 10\log\left(\frac{\ln P_d + ADT}{\ln P_d - \ln P_{fa}}\right). \tag{8}$$

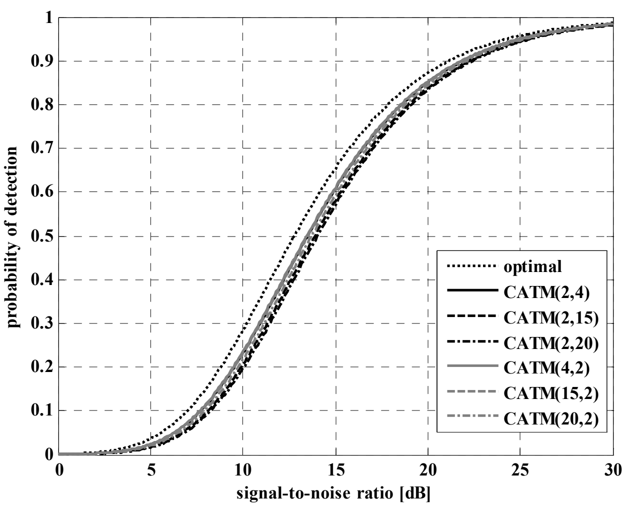

Fig. 4. Detection curves for optimal and asymmetric trimming CATM-CFAR detectors (P_{fa} = 10^{-6}, N = 24).

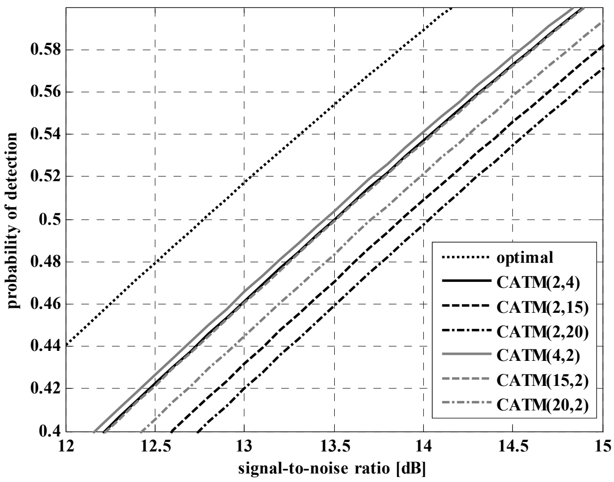

Fig. 5. Selected detection curves for optimal and asymmetric trimming CATM-CFAR detectors (P_{fa} = 10^{-6}, N = 24).

CFAR	T	ADT	Δ_O [dB]
CATM(2,4)	0.441	16.3708	0.773
CATM(2,15)	0.687	17.8563	1.166
CATM(2,20)	0.761	18.5099	1.328
CATM(4,2)	0.394	16.1757	0.718
CATM(15,2)	0.469	16.4007	0.781
CATM(20,2)	0.609	17.2001	0.996

Tab. 2. Approximate signal-to-noise ratio loss Δ_O.

Probability of detection of optimal detector, CATM, CA, TM and OS CFAR detectors as a function of the signal-to-noise ratio for parameter values from Tab. 3 are shown in Fig. 6. The notation TM(T_1,T_2) stands for TM-CFAR with lower trimming T_1 and upper trimming T_2. The notation OS(k) stands for the OS-CFAR where k [1] is well known parameter of OS-CFAR which corresponds to up mentioned trimming value. It can be seen that detection curve of the CATM-CFAR is the nearest to the detection curve of theoretically optimal detector.

CFAR	N	T_1	T_2	k	T	ADT	Δ_O [dB]
CATM	24	2	2	-	0.391	16.1727	0.717
CA	24	-	-	-	0.778	18.6787	1.369
TM	24	2	2	-	1.119	19.3756	1.534
OS	24	-	-	20	12.476	21.1175	1.921

Tab. 3. Parameter values of CFAR detectors.

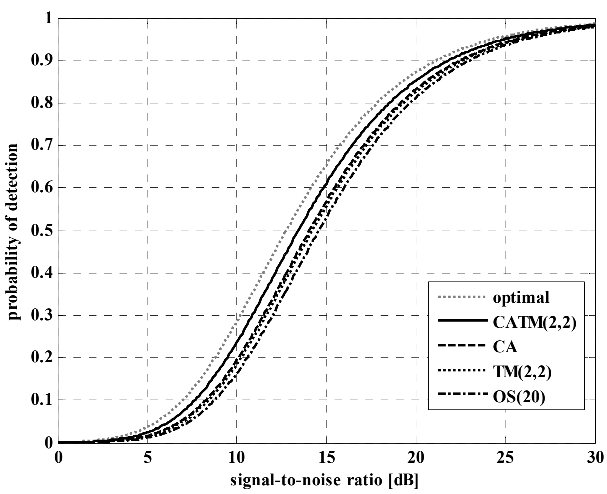

Fig. 6. Detection curves for optimal, CATM, CA, TM and OS CFAR detectors (P_{fa} = 10^{-6}, N = 24).

Fig. 7 shows average decision threshold *ADT* of CA, OS, TM and CATM CFAR detectors as a function of trimming points. As the trimming increases, *ADT* of CATM increases too. But this increase is smaller then appropriate *ADT* increase of TM-CFAR. For each value of symmetric trimming points, *ADT* of CATM-CFAR are smaller than appropriate *ADT* of TM-CFAR. Also, changes of *ADT* for asymmetric trimming by CATM-CFAR are minor in comparing with similar changes by TM-CFAR. In general, for each trimming value *k*, CATM-CFAR detector has *ADT* values that are better than those for the TM, OS and CA-CFAR detectors.

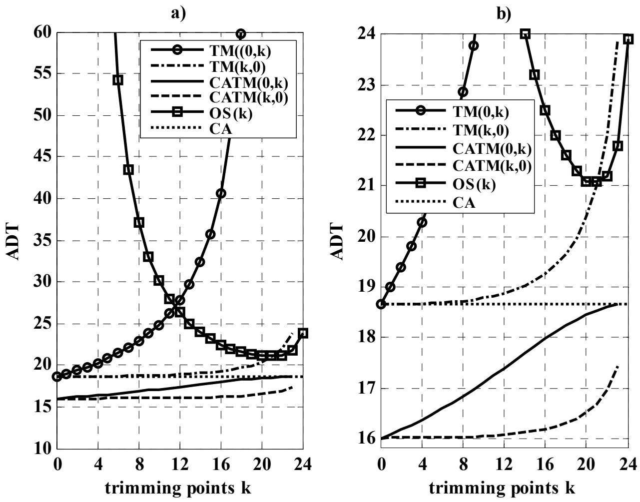

Fig. 7. Average decision threshold *ADT* of CA, OS, TM and CATM CFAR detectors ($P_{fa} = 10^{-6}$, $N = 24$).

3. CATM-CFAR False Alarm Analysis

In this section, we consider behavior of CATM-CFAR detector in presence of clutter edge. Clutter is represented here by a constant amplitude response as in [1] with constant clutter-to-noise ratio *CNR*. The model consists of two areas, clutter and background noise (Fig. 8). The incoming clutter area is extended over range cells which number is greater than reference window size *N*. The current value of the clutter edge position in reference window is marked as *R*.

Fig. 9 shows the false alarm rate performance for symmetric trimming CATM-CFAR detectors in a region of clutter power transition at $CNR = 10$ dB and desired $P_{fa} = 10^{-6}$, as a function of clutter edge position *R*, where *R* represents actually the number of successive clutter cells present in the reference window. As the reference window sweeps over the clutter edge for $R \leq n$, the probability of false alarm decreases. The P_{fa} has a sharp discontinuity at $R = n + 1$ as expected. For $R \geq n$, value of the probability of false alarm decreases toward the desired P_{fa} gradually.

In Fig. 10 it can be seen that CATM(11,11) has the lowest jump of P_{fa}, since with the increase in number of trimmed cells jump value of P_{fa} decreases.

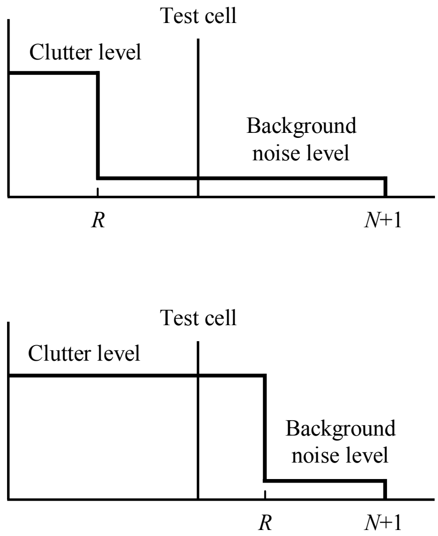

Fig. 8. Clutter model.

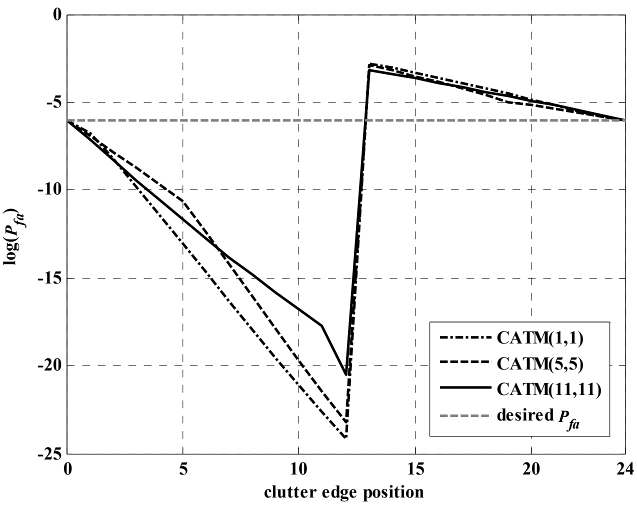

Fig. 9. False alarm rate performance for symmetric trimming CATM-CFAR in presence of clutter edge ($N = 24$).

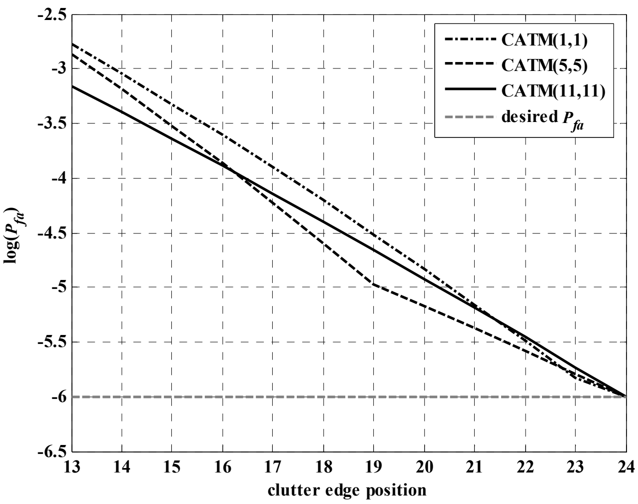

Fig. 10. Selected false alarm rate performance for symmetric trimming CATM-CFAR in presence of clutter edge ($N = 24$).

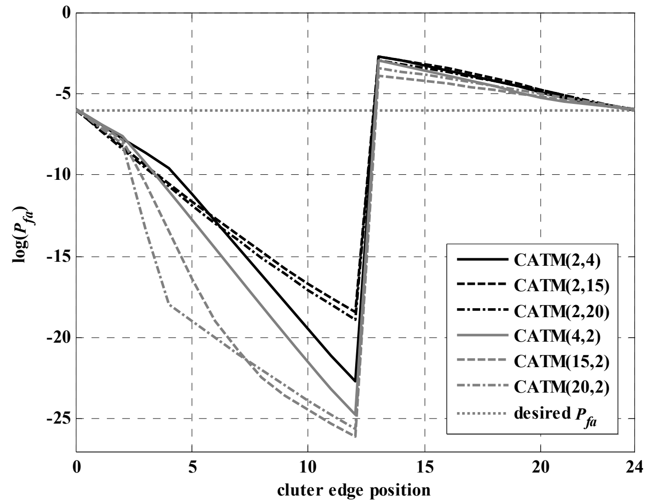

Fig. 11. False alarm rate performance for asymmetric trimming CATM-CFAR in presence of clutter edge ($N = 24$).

Next, we analyze the false alarm rate performance for asymmetric trimming CATM-CFAR detectors in presence of clutter edge with the same conditions as in the previous case. Results are shown in Fig. 11. There is a greater difference in mutual behavior at asymmetric trimming CATM-CFAR with different trimming than in case of symmetric trimming. But in general, with asymmetric trimming, trimming jump of P_{fa} for $R = n + 1$ is smaller than with symmetric trimming. In Fig. 12 it can be seen clearly that CATM(15,2) has the best false alarm performance in comparisons with considered CATM-CFAR. Change in probability of false alarm at CATM(15,2) is almost one order of magnitude smaller than at CATM(11,11). Also, in general asymmetric trimming CATM-CFAR with $T_1 > T_2$ have better false alarm performance in presence of clutter edge than those with $T_1 < T_2$.

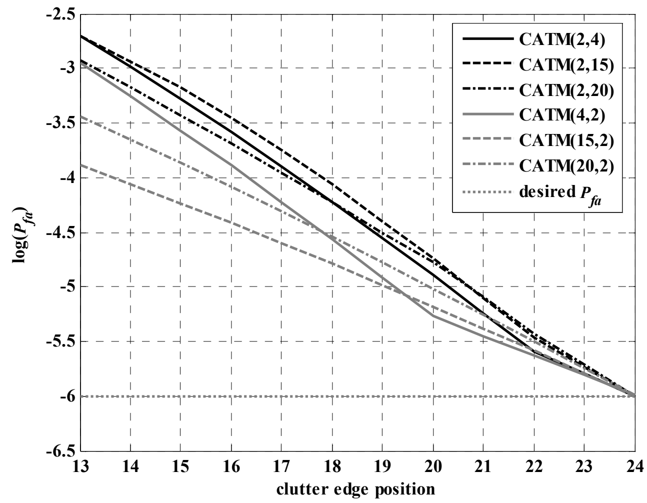

Fig. 12. Selected false alarm rate performance for asymmetric trimming CATM-CFAR in presence of clutter edge ($N = 24$).

4. Comparative False Alarm Analysis

Now, we want to compare the characteristics of the CATM-CFAR to the characteristics of well known CA-CFAR and TM-CFAR detectors in conditions of clutter power transitions for different values of *CNR* and desired P_{fa}. First, we analyzed false alarm performances for desired $P_{fa} = 10^{-6}$ and values 5 dB, 10 dB and 15 dB for *CNR*. Parameters of considered CFAR detectors are listed in Tab. 4.

CFAR	N	T_1	T_2	T	ADT	Δ_O [dB]
CATM	24	1	1	0.364	16.0833	0.692
CATM	24	6	6	0.502	16.6312	0.844
CATM	24	11	11	0.708	17.9952	1.201
CATM	24	11	0	0.359	16.0545	0.684
CATM	24	11	1	0.394	16.1371	0.707
CATM	24	11	2	0.425	16.2438	0.737
CA	24	-	-	0.778	18.6787	1.369
TM	24	2	2	1.119	19.3756	1.534

Tab. 4. Parameter values of CFAR detectors ($P_{fa} = 10^{-6}$).

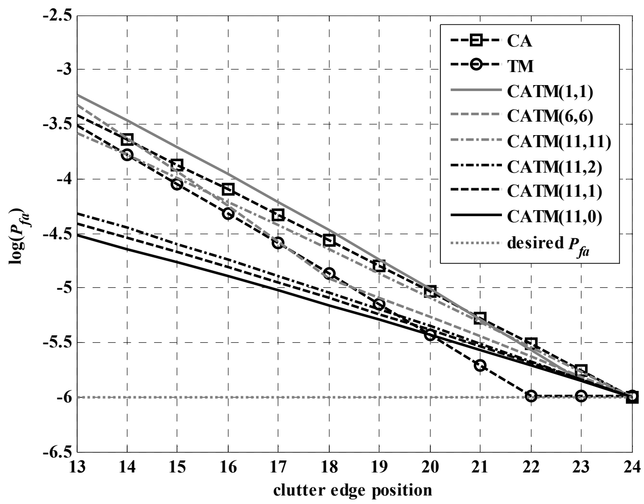

Fig. 13. Comparative false alarm analysis in presence of clutter edge (CNR = 5 dB, $P_{fa} = 10^{-6}$, $N = 24$).

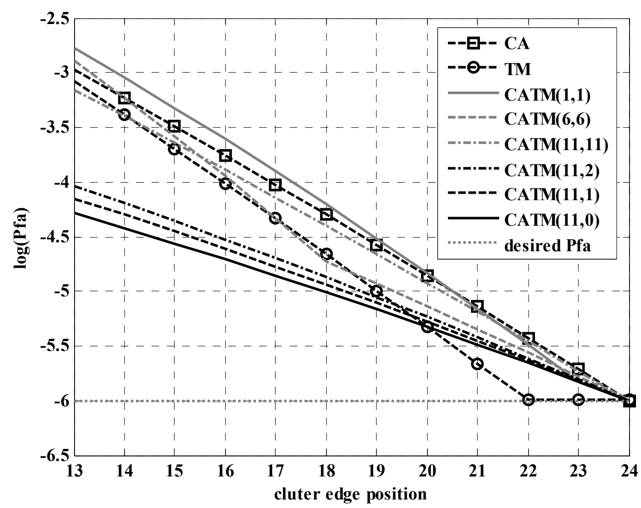

Fig. 14. Comparative false alarm analysis in presence of clutter edge (CNR = 10 dB, $P_{fa} = 10^{-6}$, $N = 24$).

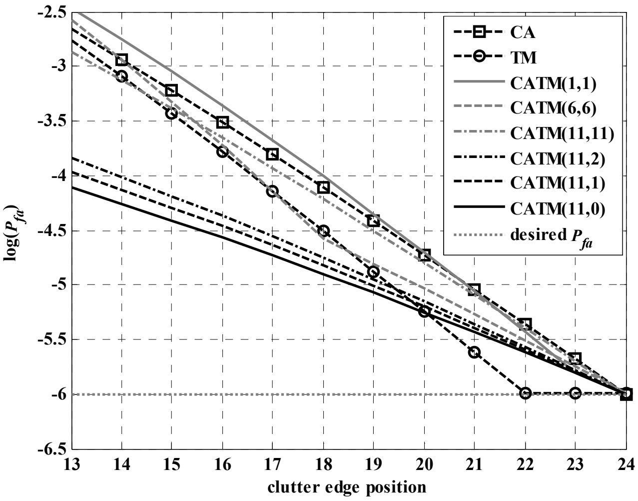

Fig. 15. Comparative false alarm analysis in presence of clutter edge (CNR = 15 dB, P_{fa} = 10^{-6}, N = 24).

In Fig. 13, 14 and 15 false alarm rate performances of considered CFAR detectors for values 5 dB, 10 dB and 15 dB for CNR are shown, respectively. As expected, abrupt changes in probability of false alarm are the least for CNR = 5 dB. CATM(11,0) for all three values of CNR gives superior results in terms of false alarm rate. Its results are almost 2 orders of magnitude better than results of CA, TM(2,2), CATM(1,1), CATM(6,6) and CATM(11,11).

Second, we analyzed false alarm performances for slightly higher desired P_{fa}=10^{-4} and CNR = 10 dB. Parameters of CFAR detectors for this case are listed in Tab. 5.

CFAR	N	T_1	T_2	T	ADT	Δ_O [dB]
CATM	24	1	1	0.231	10.1846	0.470
CATM	24	6	6	0.315	10.4158	0.575
CATM	24	11	11	0.432	10.9713	0.816
CATM	24	11	0	0.227	10.1731	0.465
CATM	24	11	1	0.249	10.2081	0.481
CATM	24	11	2	0.269	10.2535	0.502
CA	24	-	-	0.468	11.2272	0.923
TM	24	2	2	0.664	11.4944	1.032

Tab. 5. Parameter values of CFAR detectors (P_{fa} = 10^{-4}).

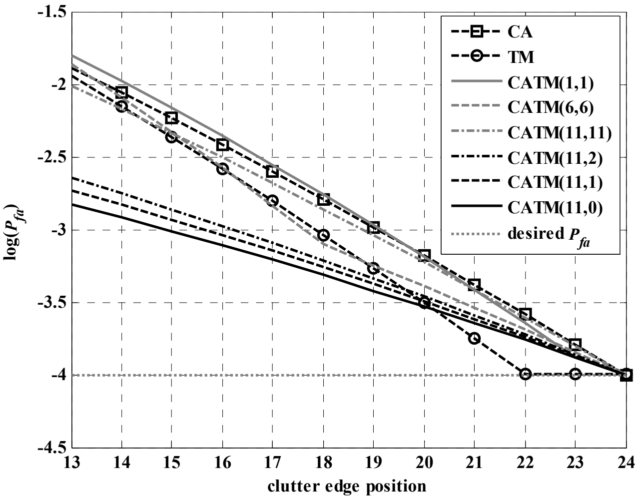

Fig. 16. Comparative false alarm analysis in presence of clutter edge (CNR = 10 dB, P_{fa} = 10^{-4}, N = 24).

Results of calculated values of P_{fa} are shown in Fig. 16. Situation is similar like before the increase of desired P_{fa}. CATM(11,0) has superior results of false alarm rate again, but in this case, its results are roughly one order of magnitude better than results of CA, TM(2,2), CATM(1,1), CATM(6,6) and CATM(11,11). Furthermore, it can be noticed in Tab. 4 and 5 that CATM(11,0) has the least signal-to-noise ratio losses relatively to another considered CFAR models. Therefore, its detection performance will be the best, too.

5. Conclusion

It was shown earlier [8] that CATM-CFAR gives excellent results in terms of probability of detection and values of average decision threshold.

In this paper false alarm analysis of CATM-CFAR in presence of clutter edge of the clutter with constant amplitude response is performed. Scenarios with different clutter-to-noise ratio and desired probability of false alarm are discussed.

Analysis has shown that with a proper choice of trimming parameters, CATM can have even two orders of magnitude better results in case of undesired false alarm rate variations in presence of clutter edge than some other well known CFAR models. The better clutter edge characteristic is achieved without compromising the probability of detection.

Direction of further research would be moving toward an examination of characteristics of the realized CATM-CFAR detector under conditions of presence of Weibull, Rice or some another clutter edge and its effect on detection of radar targets.

Acknowledgements

This work was partially supplied by the Ministry of Education, Science and Technological Development of the Republic of Serbia under Grants III-47029.

References

[1] ROHLING, H. Radar CFAR thresholding in clutter and multiple target situations. *IEEE Trans. Aerosp. Electron. Syst.*, 1983, vol. 19, p. 608–621.

[2] HANSEN, H. M. Constant false alarm rate processing in search radar. In *Proceedings of the IEE International Radar Conference*. London (UK), Oct. 1979, p. 325-332.

[3] HANSEN, G. V., SAWYERS, J. H. Detectability loss due to greatest-of selection in a cell averaging CFAR. *IEEE Trans. Aerosp. Electron. Syst.*, 1980, vol. 16, p. 115–118.

[4] RICKARD, J. T., DILLARD, G. M. Adaptive detection algorithms for multiple target situations. *IEEE Trans. Aerosp. Electron. Syst.*, 1977, vol. 13, no. 4, p. 338–343.

[5] GANDHI, P. P., KASSAM, S. A. Analysis of CFAR processors in nonhomogenous background. *IEEE Trans. Aerosp. Electron. Syst.*, 1988, vol. 24, no. 4, p. 427–445.

[6] ZAIMBASHI, A., TABAN, M. R., NAYEBI, M. M., NOROUZI, Y. Weighted order statistic and fuzzy rules CFAR detector for Weibull clutter. *Signal Processing*, 2008, vol. 88, p. 558–570.

[7] POURMOTTAGHI, A., TABAN, M. R., GAZOR, S., A CFAR detector in a nonhomogenous Weibull clutter. *IEEE Trans. Aerosp. Electron. Syst.*, 2012, vol. 48, no. 2, p. 1747 – 1758.

[8] IVKOVIĆ, D., ANDRIĆ, M., ZRNIĆ, B. A new model of CFAR detector. *Frequenz - Journal of RF-Engineering and Telecommunications*, DOI 10.1515/freq-2013-0087, Jan. 2014.

About Authors …

Dejan IVKOVIĆ was born in Smederevo in Serbia in 1972. He received the B.Sc. degree in Electronics Engineering from the Military Technical Academy, Serbia in 1996. He received his M.Sc. in Telecommunication from the School of Electrical Engineering, University of Belgrade in 2006. Currently, he works as a researcher at the Radar Systems Laboratory of the Military Technical Institute in Belgrade. His research interests include digital processing of radar signals, software radar receiver and algorithms of constant false alarm rate detectors of radar targets. He has published 23 papers in national and international conferences and journals to date.

Milenko ANDRIĆ was born in Pljevlja in 1972, Montenegro. He received the B.Sc. degree in Electronics Engineering from the Military Technical Academy, Serbia in 1995. He received his M.Sc. in Telecommunication from the School of Electrical Engineering, University of Belgrade, Serbia in 2001. He received the PhD degree in Military Electronic Systems from the Military Academy, University of Defense in Belgrade, Serbia in 2006. Currently, he is an associate professor at the Department of Military Electronics Engineering and he works also as a researcher at the Electronic Systems Laboratory of the Military Academy in Belgrade. His main research interests are in the fields of stochastical process in telecommunication and radar engineering, pattern recognition, methods for signal analysis and digital signal processing. He has published more than 50 papers in national and international conferences and journals to date.

Bojan ZRNIĆ graduated in 1992 on the Military Technical Academy in Belgrade with B.Sc. degree in Electrical Engineering. He received M.Sc. and Ph.D. in Electrical Engineering in 1998 and 2001, respectively. Currently, he is the Head of Defense Technology Department in Serbian MOD. He is also visiting professor at the Serbian Military Academy on the radar and EW subjects. His research work includes radar signals and systems. He published over 70 papers in national and international conference proceedings and journals.